17th World Conference on Earthquake Engineering, 17WCEE
Sendai, Japan - September 13th to 18th 2020

LATERAL LOAD ANALYSIS OF ROCKING WALL-MOMENT FRAME SYSTEMS CONSIDERING AXIAL DEFORMATION OF COLUMNS

N. Subedi[(1)], A. C. Wijeyewickrema[(2)], S. Kono[(3)]

[(1)] *Graduate Student, Tokyo Institute of Technology, subedi.n.aa@m.titech.ac.jp*
[(2)] *Associate Professor, Tokyo Institute of Technology, Japan, wijeyewickrema.a.aa@m.titech.ac.jp*
[(3)] *Professor, Tokyo Institute of Technology, Japan, kono.s.ae@m.titech.ac.jp*
…

Abstract

Considerable damage to reinforced concrete walls during strong earthquakes has led to the development of innovative precast concrete walls known as rocking walls that can uplift and rock about their base. These walls may be equipped with energy dissipating elements to limit damage to the structural components and post-tensioning to provide self-centering capability. The benefits of rocking walls can also be utilized in rocking wall-moment frame (RWF) systems, where the moment frame and rocking wall share the total gravity loads and design seismic forces. Previous analytical studies of the lateral load response of RWF systems have simplified the frame as an equivalent shear cantilever with no axial deformations (assuming axially-rigid columns). However, for tall and slender frames, axial extension and shortening of the columns cause global bending and associated lateral displacement of the structure cannot be ignored. The present study addresses this by extending the analytical solution to include the contribution from axial deformation of columns. Closed-form solutions for the lateral deformation, shear force, and bending moment are obtained for typical loading profiles. The accuracy of the proposed solutions is verified with the results from detailed finite element analysis. These solutions are then utilized to investigate the influence of axial deformation of frames, relative stiffness between frame and wall, and wall base restraint on the response of the RWF system. The results show that axial deformation of columns increases overall displacement and drift of the RWF system. These effects are more pronounced for higher frame-to-wall stiffness ratios where the frame controls the overall system response.

Keywords: analytical model; axial deformation; lateral load analysis; rocking wall.

1. Introduction

In recent years, seismic design codes and standards are focused on improving the seismic resilience of structural systems with minimal damage to structural components. Considerable damage suffered by conventional lateral load resisting systems (such as moment-resisting frames, wall-frame, and braced frames) during strong earthquakes, has led to the development of "sustainable" earthquake-resisting systems capable of limiting structural damage, self-centering, and replacement of the damaged components after severe earthquakes.

The concept of rocking (gap opening/closing at the base) was rediscovered as a means to limit structural damage and facilitate re-centering after earthquakes. Based on this concept, several structural systems that can uplift and rock about their base have been developed. Examples of such systems include precast rocking walls [1-4], rocking steel-braces [5, 6], post-tensioned timber walls [7], etc. These rocking systems can be equipped with energy dissipating (ED) elements to limit damage to the structural components and post-tensioning (PT) to provide self-centering capability. A rocking wall-moment frame (RWF) combines rocking walls with a moment-resisting frame to achieve a low-damage structural system. In a RWF system, the rocking wall mitigates drift concentrations in a particular story by enforcing uniform drift distribution [8] and prevents damage to the structural members by concentrating damage in the replaceable ED elements [3].

With the growing interest in rocking systems, simplified analytical models are being developed to estimate the distribution of seismic demands in RWF buildings [9-11]. In such models, the RWF assembly is idealized as a combination of substitute beams and earthquake loading is represented by distributed lateral force. Governing equations are formulated utilizing equilibrium of forces and compatibility of displacements, and solved for different loading conditions. Analytical solutions are useful to understand the seismic behavior of RWF systems for preliminary design or rapid performance evaluation where detailed modeling is dispensable.

In a laterally loaded RWF system, the rocking wall deforms in flexural mode and frames deflect predominantly in a shear-mode profile [9, 10]. Accordingly, Pan et al. [9] idealized the pinned-wall frame (PWF) system (pinned-wall meaning a rocking wall with no rotational restraint at the base) as a coupled-two-beam model consisting of a shear beam and a flexural beam, representing the frame and the wall, respectively. These beams are connected by continuous rigid links to deflect equally at each level. Governing equations were derived assuming uniform wall-frame and axially-rigid columns. Expressions for lateral displacement, moment, and shear force distribution were obtained for uniformly distributed load, inverted triangular load, and a point load at the top and the analytical solutions were verified with the results from finite element analysis. Following a similar approach, the lateral load behavior of RWF system was studied by Rahgozar et al. [10], by introducing a rotational spring at the base of flexural beam to account for variable moment-restraint provided by PTs, ED devices, and self-weight of the rocking wall. Sun et al. [11] extended the model of Pan et al. [9] to include the effect of distributed dampers between the pinned-wall and frames. They showed that the addition of dampers in the system affects shear force and moment distribution of the pinned-wall.

In all of these studies, columns in RWF are assumed to be axially-rigid and the moment-frame is simplified as an equivalent shear cantilever. However, for tall and slender frames, axial extension and shortening of the columns cause global bending and associated lateral displacement of the structure can be considerable. Sun et al. [11] investigated how the assumption of infinite column axial stiffness affects the accuracy of analytical solution. Based on the prediction errors, they concluded that their solution cannot be applied for high-rise PWF structures as the contribution from axial deformation of columns is non-negligible. Therefore, there is a need to revise the existing formulation.

The present study is an extended formulation for the lateral load analysis of a RWF system which includes the contribution from axial deformation of columns. Closed-form solutions for the lateral deformation, shear force, and bending moment are obtained for three typical loading profiles. Solutions

obtained herein are applicable for both pinned-wall [9,11] and post-tensioned *hybrid* rocking core [3, 4, 6, 7] configurations reported in the literature. Accuracy of the proposed solutions is verified with the results from detailed finite element analysis. Then, the validated solutions are utilized to investigate the influence of axial deformation of frames, relative stiffness between frame and wall, and wall base restraint on the RWF response.

2. Distributed Parameter Model for a Rocking Wall-Moment Frame (RWF) System

2.1 Assumptions of the model

For the analytical solution, a planar RWF system is represented by a coupled two-beam model as shown in Fig. 1(a). The governing equation for the RWF is based on following assumptions:

(a) The moment-frame is represented by an elastic beam with both shear and flexural deformations. An "effective" flexural deformation component is introduced to incorporate the lateral deformation resulting from axial deformability of columns.

(b) The rocking wall is represented by an elastic flexural beam neglecting shear deformations.

(c) The frame (columns, beams) and wall have uniform properties over the height.

(d) Lateral loads are distributed along the height and the discrete set of connecting members are replaced by a continuous connecting medium. All discrete forces are idealized as distributed forces.

2.2 Analytical solution for the coupled two-beam model of the RWF system

For a laterally loaded RWF system, equilibrium of interaction forces and deformation compatibility are utilized to derive the governing equation.

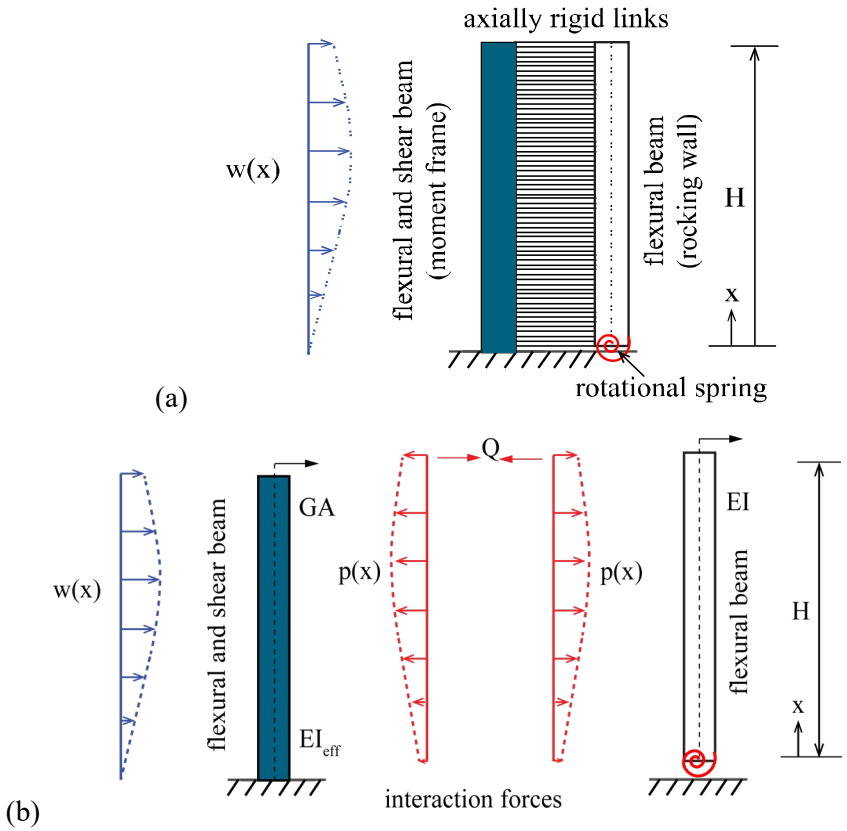

Fig. 1 – Schematic of: (a) coupled two-beam model for RWF system, and (b) system of interaction forces.

Referring to the system of interaction forces in Fig. 1(b), the shear force in the flexural beam (rocking wall) can be written as [12],

$$V_w(x) = -EI\frac{d^3y}{dx^3} = \int_x^H p(x)dx - Q, \tag{1}$$

where x represents position along the height, EI is the flexural stiffness of rocking wall, y is the lateral deflection of the flexural beam, $p(x)$ is the distributed interaction force, Q is the interaction force at the roof level, and H is the building height.

For the flexural and shear beam (moment frame), total curvature is taken as the summation of: (a) curvature resulting from racking (shear-type) deformation of frames $\frac{d^2y_{s1}}{dx^2}$ and (b) curvature from axial deformation of columns $\frac{d^2y_{s2}}{dx^2}$ [13] i.e.,

$$\frac{d^2y}{dx^2} = \frac{d^2y_{s1}}{dx^2} + \frac{d^2y_{s2}}{dx^2}, \tag{2}$$

where y_{s1} and y_{s2} are the lateral displacements of frame resulting from the racking and axial deformations, respectively. To obtain the racking component, the shear force on the flexural and shear beam (Fig. 1(b)) can be expressed as [12],

$$GA\frac{dy_{s1}}{dx} = \int_x^H [w(x) - p(x)]dx + Q, \tag{3}$$

where $w(x)$ is the distributed external load and the racking rigidity GA is defined as the shear force required to cause unit story drift in the frame (Smith and Coull [14], Chapter 7),

$$GA = \frac{12E}{h_i\left(\frac{1}{\Sigma(I_c/h)_i} + \frac{1}{\Sigma(I_b/l)_i}\right)}, \tag{4}$$

where E is the Young's modulus of the moment frame, h_i is the story height, l is the bay width, I_c and I_b are moments of inertia of column and beam, respectively.

The external moment on the shear beam $M_s(x)$ is related to the curvature resulting from the axial deformation of the columns and is given by,

$$M_s(x) = EI_{eff}\frac{d^2y_{s2}}{dx^2}, \tag{5}$$

where EI_{eff} is the *effective flexural stiffness* of the frame which accounts for the axial deformability of the columns and is given by,

$$EI_{eff} = E\Sigma A_i c_i^2, \tag{6}$$

and $\Sigma A_i c_i^2$ is the sum of the second moments of area of the column sectional area A_i about their common center of area c_i [13].

Substituting Eqs. (3) and (5) in Eq. (2) yields,

$$-GA\left(\frac{d^2y}{dx^2}-\frac{M_s(x)}{EI_{eff}}\right)=w(x)-p(x). \tag{7}$$

Hence, $M_s(x)$ can be obtained using the external moment due to applied load $M_{Ext.}(x)$ and moment on the rocking wall $M_w(x)$ as,

$$M_s(x)=M_{Ext.}(x)-EI\frac{d^2y}{dx^2}. \tag{8}$$

Differentiating Eq. (1) and combining with Eqs. (7) and (8), yields the governing equation for the lateral deformation of the RWF system as,

$$\frac{d^4y}{d\xi^4}-(\alpha k)^2\frac{d^2y}{d\xi^2}=\frac{H^4}{EI}\left(w(\xi)-\frac{\alpha^2}{H^2}(k^2-1)\int_{\xi}^{1}\int_{z}^{1}w(\xi)H^2d\xi dz\right), \tag{9}$$

where $\xi=x/H$ is the normalized height, α and k are frame-to-wall stiffness and axial stiffness parameters for the RWF system defined as,

$$\alpha=\sqrt{\frac{GA}{EI}}H \quad \text{and} \quad k=\sqrt{1+\frac{EI}{EI_{eff}}}. \tag{10}$$

The governing equation for the lateral deformation of RWF system (Eq. (9)) differs from that of Rahgozar et al. [10] and Sun et al. [11] due to the introduction of axial stiffness parameter k. For the case of axially-rigid columns, ($EI_{eff} >> EI$) $k=1$, this equation reduces to the governing equation of existing studies [10, 11]. Note that for *RWF system with distributed dampers* along the height an additional restraining moment is exerted on the wall by the dampers. To incorporate this contribution from the dampers, the parameters α and k can be defined as,

$$\alpha=\sqrt{\frac{GA+C_{eq}}{EI}}H, \quad \text{and} \quad k=\sqrt{1+\frac{GA}{GA+C_{eq}}\frac{EI}{EI_{eff}}}, \tag{11}$$

where C_{eq} is equivalent damper stiffness, defined as [11],

$$C_{eq}=\frac{A_dG_dl_w^{\,2}}{2a_d\bar{h}}, \tag{12}$$

where A_d is the effective shear area of dampers, G_d is the elastic shear modulus for the dampers, l_w is the wall length, a_d is the damper length (between the wall and frame), and $\bar{h}$ is the average story height.

The distributed lateral force on the RWF system $w(\xi)$ can be expressed in a general form which can represent load patterns ranging from uniform to parabolic distributions (similar to equivalent seismic/wind force distribution in design codes) as,

$$w(\xi)=w_0\xi^n, \tag{13}$$

where w_0 is the intensity of loading at the top and n is a non-dimensional parameter that accounts for the distribution of lateral forces along the height ($n=0$ for uniform loading; $n=1$ for inverted triangular loading).

The solution of Eq. (9) can be expressed as,

$$y(\xi)=C_1+C_2\xi+C_3\sinh(\alpha k\xi)+C_4\cosh(\alpha k\xi)+y_0(\xi), \tag{14}$$

where $y_0(\xi)$ is the particular solution and $C_i (i = 1,...4)$ are arbitrary constants.

The relevant boundary conditions are,

(a) Lateral deformation at the base is zero,

$$y(0) = 0. \tag{15}$$

(b) Moment at the base of rocking wall is defined in terms of nondimensional rotational stiffness R_f as [10],

$$M_w(0) = \frac{EI}{H^2}\frac{d^2y}{d\xi^2}\bigg|_{\xi=0} = R_f \frac{EI}{H^2}\frac{dy}{d\xi}\bigg|_{\xi=0}, \tag{16}$$

where $R_f = \dfrac{k_w H}{EI}$; and k_w is the stiffness of rotational spring at wall base defined as,

$$k_w = k_{PT,\sec} + k_{ED,\sec} + k_{AW,\sec} = \frac{1}{\phi_w}\left(M_{PT,\phi} + M_{ED,\phi} + M_{AW,\phi}\right), \tag{17}$$

where $M_{PT,\phi}$, $M_{ED,\phi}$, and $M_{AW,\phi}$ are the moment contributions from the PT tendons, ED elements, and axial load on the wall at roof drift ϕ_w. Note that this boundary condition is capable of representing wall base restraint ranging from pinned state when $R_f = 0$ to the fully fixed state when $R_f \to \infty$.

(c) Moment at the top of rocking wall is zero,

$$M_w(1) = \frac{EI}{H^2}\frac{d^2y}{d\xi^2}\bigg|_{\xi=1} = 0. \tag{18}$$

(d) The total shear force at the top is zero,

$$-\frac{d^3y}{d\xi^3}\bigg|_{\xi=1} + (\alpha k)^2 \frac{dy}{d\xi}\bigg|_{\xi=1} - \alpha^2(k^2-1)\frac{dy}{d\xi}\bigg|_{\xi=0} - \frac{\alpha^2}{EI}(k^2-1)H\int_0^1\int_\xi^1\int_z^1 w(\xi)H^3 d\xi dz d\xi = 0. \tag{19}$$

The moment $M_w(\xi)$ and shear force $V_w(\xi)$ in the rocking wall can be computed from,

$$M_w(\xi) = \frac{EI}{H^2}\frac{d^2y}{d\xi^2}, \tag{20}$$

and

$$V_w(\xi) = -\frac{EI}{H^3}\frac{d^3y}{d\xi^3}. \tag{21}$$

As noted earlier, for a RWF system with distributed dampers along the height, the total shear force carried by the wall V_w^{tot} should include the contribution from the dampers, i.e., $V_w^{tot} = V_w(\xi) + m(\xi)$, where $m(\xi)$ is the shear force resisted by the dampers.

The moment $M_f(\xi)$ and shear force $V_f(\xi)$ in the moment frame can be obtained from,

$$M_f(\xi) = M_{Ext.}(\xi) - M_w(\xi), \tag{22}$$

and

$$V_f(\xi) = V_{Ext.}(\xi) - V_w(\xi). \tag{23}$$

where $M_{Ext.}(\xi)$ and $V_{Ext.}(\xi)$ are the moment and shear force due to the applied external lateral force $w(\xi)$.

2.2.1 Uniformly distributed loading

For a uniformly distributed load, $w(\xi) = w_0$ and $M_{Ext.}(\xi) = \frac{w_0 H^2}{2}(1-\xi)^2$. Using the boundary conditions Eqs. (15)-(19),

$$C_1 = -C_4 = \frac{w_0 H^4}{2EI} \frac{\left[-2kR_f \operatorname{sech}(\alpha k) + \alpha \tanh(\alpha k)\left(-2 + k^2\left(-2R_f + \alpha^2(k^2-1)\right)\right)\right]}{\alpha^4 k^6 \left[kR_f + \alpha \tanh(\alpha k)\right]}, \tag{24}$$

$$C_2 = \frac{w_0 H^4}{2EI} \frac{\left[\cosh(\alpha k)\left(2 + k^2\left(-2 + 2R_f + \alpha^2(k^2-1)^2\right)\right) + 2\left(-1 + k^2 + \alpha k^3 \sinh(\alpha k)\right)\right]}{\alpha^2 k^5 \left(kR_f \cosh(\alpha k) + \alpha \sinh(\alpha k)\right)}, \tag{25}$$

$$C_3 = \frac{w_0 H^4}{2EI} \frac{\left[2 + \cosh(\alpha k)\left(-2 + k^2\left(-2R_f + \alpha^2\left(k^2-1\right)\right)\right)\right]}{\alpha^3 k^6 \left(kR_f \cosh(\alpha k) + \alpha \sinh(\alpha k)\right)}, \tag{26}$$

$$y_0(\xi) = -\frac{w_0 H^4}{4EI} \frac{[2-(\alpha k)^2(k^2-1)]}{\alpha^2 k^4} \xi^2 - \frac{w_0 H^4}{6EI} \frac{(k^2-1)}{k^2} \xi^3 + \frac{w_0 H^4}{24EI} \frac{(k^2-1)}{k^2} \xi^4. \tag{27}$$

2.2.2 Inverted triangular loading

For an inverted triangular load, $w(\xi) = w_0 \xi$ and $M_{Ext.}(\xi) = \frac{w_0 H^2}{6}(2 - 3\xi + \xi^3)$; where w_0 is the load intensity at the top. Using the boundary conditions Eqs. (15)-(19),

$$C_1 = -C_4 = \frac{w_0 H^4}{6EI} \frac{\left[\operatorname{sech}(\alpha k)\left(-6\alpha k R_f + \left(2\alpha^4 k^2\left(k^2-1\right) + R_f\left(6 - 3\alpha^2 k^2\right)\right)\sinh(\alpha k)\right)\right]}{\alpha^5 k^6 \left(kR_f + \alpha \tanh(\alpha k)\right)}, \tag{28}$$

$$C_2 = \frac{w_0 H^4}{6EI} \frac{\left[\cosh(\alpha k)\left(2\alpha^4 k^2\left(k^2-1\right)^2 + 3R_f\left(\alpha^2 k^2 - 2\right)\right) + 3\alpha\left(2\alpha(k^2-1) + k\sinh(\alpha k)\left(\alpha^2 k^2 - 2\right)\right)\right]}{\alpha^4 k^5 \left(kR_f \cosh(\alpha k) + \alpha \sinh(\alpha k)\right)}, \tag{29}$$

$$C_3 = \frac{w_0 H^4}{6EI} \frac{\left[6\alpha^2 + \cosh(\alpha k)\left(2\alpha^4 k^2\left(k^2-1\right) + R_f\left(6 - 3\alpha^2 k^2\right)\right)\right]}{\alpha^5 k^6 \left(kR_f \cosh(\alpha k) + \alpha \sinh(\alpha k)\right)}, \tag{30}$$

$$y_0(\xi) = \frac{w_0 H^4}{6EI} \frac{(k^2-1)}{k^2} \xi^2 - \frac{w_0 H^4}{12EI} \frac{\left[2 + (\alpha k)^2(k^2-1)\right]}{\alpha^2 k^4} \xi^3 + \frac{w_0 H^4}{120EI} \frac{(k^2-1)}{k^2} \xi^5. \tag{31}$$

2.2.3 Concentrated force at top

For a concentrated force p_0 at the top: $w(\xi) = 0$ and $M_{Ext.}(\xi) = p_0 H(1-\xi)$. Using the boundary conditions Eqs. (15)-(19),

$$C_1 = -C_4 = -\frac{p_0 H^3}{EI}\frac{\left[R_f - \alpha^2\left(k^2-1\right)\right]\sinh(\alpha k)}{\alpha^3 k^4\left(kR_f\cosh(\alpha k)+\alpha\sinh(\alpha k)\right)}, \tag{32}$$

$$C_2 = \frac{p_0 H^3}{EI}\frac{\left[\left(R_f + \alpha^2(k^2-1)^2\right)\cosh(\alpha k)+\alpha k\sinh(\alpha k)\right]}{\alpha^2 k^3\left(kR_f\cosh(\alpha k)+\alpha\sinh(\alpha k)\right)}, \tag{33}$$

$$C_3 = -\frac{p_0 H^3}{EI}\frac{\left[R_f - \alpha^2\left(k^2-1\right)\right]\cosh(\alpha k)}{\alpha^3 k^4\left(kR_f\cosh(\alpha k)+\alpha\sinh(\alpha k)\right)}, \tag{34}$$

$$y_0(\xi) = \frac{p_0 H^3}{2EI}\frac{(k^2-1)}{k^2}\xi^2 - \frac{p_0 H^3}{6EI}\frac{(k^2-1)}{k^2}\xi^3. \tag{35}$$

2.3 Validation of the analytical coupled two-beam model for the RWF system

To verify the accuracy of the proposed solution, the analytical response predictions are compared with the results obtained by using a detailed finite element model using OpenSees [15]. For this purpose, results under inverted triangular load are compared for the five-bay pinned-wall frame used in Sun et al. [11]. The building has a story height of 3 m (except for the bottom story) with beam and column section dimensions of $300\times600\,\text{mm}^2$ and $650\times650\ \text{mm}^2$, respectively. The 20-story variant of the original frame is utilized for the validation, as the contribution from axial deformation of columns is expected to be non-negligible for tall and slender frames. The elastic modulus of moment frame is taken as 30000 MPa and the height of first story is increased to 5.4 m so as to result in similar shear stiffness of 4.22×10^5 kN along each story. Metallic dampers are placed at each floor level wall-to-frame connections. The properties of pinned-wall and dampers are determined to give $\alpha = 1.9$ and $\lambda = 0.7$ (where $\lambda = C_{eq}/GA$, is the ratio of equivalent damper stiffness to moment frame stiffness). As described in Sun et al. [11], the moment frame and pinned-wall are modeled as linear-elastic beam-column elements. The dampers are modeled using zero-length elements. Lateral loads are applied at the floor levels in the finite element model as opposed to the distributed loading in the analytical model. Note that, unlike Sun et al. [11], the axial deformation of columns is not restrained in the numerical model.

The lateral displacement, shear force and bending moment distribution in the pinned-wall predicted by the analytical solution are compared with the finite element results in Fig. 2. The intensity of inverted triangular loading w_0 used in the analytical solution is calculated to maintain identical total force as in the numerical model. Displacements and moments from the OpenSees [15] model are plotted at each floor level, whereas the shear force is plotted at the center of each story. Bending moment at each floor level is computed as the average of moments at the connecting nodes of the wall elements above and below that level. Wall shear and moments are normalized by total external base shear and base moment, respectively. Predictions using analytical solutions of Sun et al. [11] where the columns are considered axially-rigid are also included for comparison.

The analytical predictions are in reasonable agreement with the OpenSees [15] results (Fig. 2). Displacement predictions from the proposed solution and that of Sun et al. [11] diverge for tall buildings due to the contribution from axial deformation of columns. The discrepancy observed for wall shear force at the first story (Fig. 2(b)) is due to the larger stiffness of the bottom story of the moment frame resulting from the fixed boundary condition, thus causing the wall to take less shear force at the first story. The solution presented herein results in better predictions of the lateral displacement (Fig. 2(a)) and moment distribution (Fig. 2(c)) in the wall. Therefore, the proposed solution can reliably predict the lateral load response of RWF buildings within the linear-elastic range. Other validation examples, details regarding the numerical modeling, and story-stiffness calculations can be found in Subedi [16].

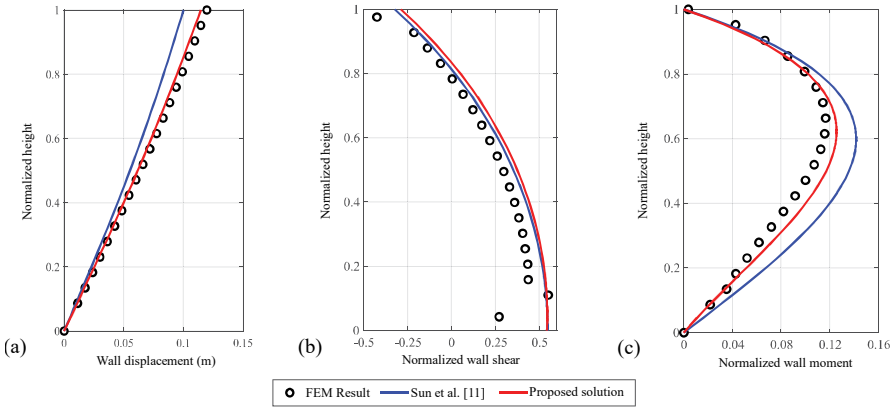

Fig. 2 – Comparison of response predictions using the proposed solution, existing solution [11], and FEM numerical model; for a 20-story pinned wall-frame system with metallic dampers placed at each floor level wall-to-frame connection: (a) lateral displacement, (b) normalized wall shear, and (c) normalized wall moment.

3. Application of Proposed Solution

The validated analytical solutions are utilized in this section to investigate the influence of axial deformation of moment frames, relative stiffness between frame and wall, and wall base restraint. For brevity, only representative results for the combinations of frame-to-wall relative stiffness $\alpha = 1, 6$, base rotational stiffness parameter $R_f = 0, 10,$ and axial stiffness parameter $k = 1, 1.02, 1.04, 1.06,$ under inverted triangular loading are presented herein. A small α (e.g., $\alpha = 1$) represents a RWF system with a stiff wall, whereas a large α (e.g., $\alpha = 6$) means a relatively flexible wall. Fig. 3 shows the lateral displacement profile, drift ratio, shear force, and moment distribution in the rocking wall. To enable a more meaningful comparison, lateral displacements and drifts are normalized by the roof displacement $y(1)$ and roof drift $y(1)/H$ corresponding to axially-rigid columns (i.e, $k = 1.0$). The wall shear force and wall moment are normalized by the total base shear and total base moment, respectively.

For a RWF system with relatively stiff wall $(\alpha = 1)$, the displacements, drifts, shear force and moment distributions are practically unaffected by the axial stiffness parameter k (Fig. 3). This is because the overall RWF system response is controlled by the wall and the constraining forces from the frame are relatively small. An overall increase in system lateral deformation is observed, as expected, when axial deformability of columns is considered [Fig. 3(a)]. Increasing the base restraint R_f affects the displacement profile of the RWF system. For a pinned wall $(R_f = 0)$, the RWF deforms in a rigid-body rotation mode resulting in a linear displacement profile and uniform drift along the height. However, for higher R_f values displacements and drifts in the bottom half are reduced and the RWF deforms in a flexural profile similar to a "conventional" fixed-base wall, with maximum drift occurring near the roof level. Shear force and moments carried by the wall increases markedly with R_f, with the wall taking most of the applied load.

In contrast, for a RWF with relatively flexible wall $(\alpha = 6)$, the displacement and force demands are notably affected by the axial stiffness parameter k. In this case, RWF system response is controlled by the moment frame and a change in effective flexural stiffness of frames is reflected in the response. A moment frame with higher k values results in greater lateral displacements and drifts, owing to increased contributio-

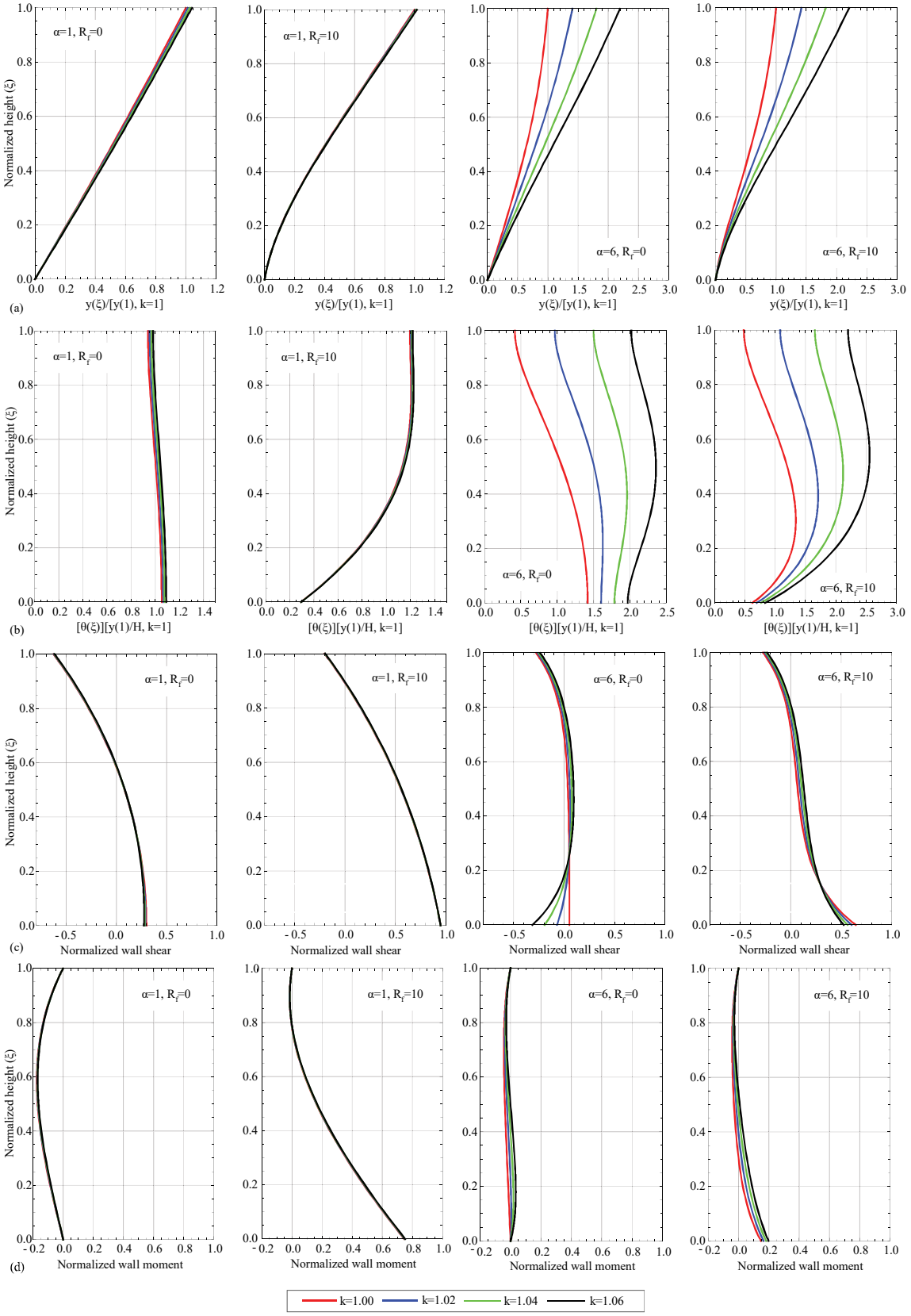

Fig. 3 – Effect of axial stiffness parameter k and base rotational stiffness parameter R_f on normalized: (a) lateral displacement, (b) lateral drift, (c) wall shear force, and (d) wall moment.

-on from axial deformation of columns. Parameter k also influences the lateral drift profile of the RWF system. When axial deformations are not significant (i.e., $k = 1$) the maximum drift always occurs at the bottom story as in pure shear-type frames. In contrast, for $k > 1.0$, an overall increase in drifts is observed with maximum drift location gradually shifting to the upper levels. The moment and shear force carried by the wall increase with increasing k, accompanied by corresponding decrease in frame moment and shear. An increase in k causes corresponding increase in wall base shear force (negative shear value) forcing the frame to carry shear forces greater than total applied shear force at the base. This implies that ignoring the contribution from axial deformation of the frame can lead to nonconservative estimates of forces and deformation parameters for the RWF system with a relatively flexible wall. Similar to the stiff wall case, an increase in base restraint R_f causes the displacements and drifts to reduce in the bottom half of the RWF system. Shear force and moment carried by the wall increases markedly near the base with increase in R_f.

4. Conclusions

In order to study the seismic behavior of RWF systems, an analytical method is presented for lateral load analysis of uniform RWF systems, including the contribution from axial deformation of columns. Closed-form solutions of the lateral deformation were presented for uniform loading, inverted triangular loading, and concentrated force at the top. The accuracy of the proposed solutions was verified with finite element analysis results. A systematic parametric analysis was carried out to understand the influence of axial stiffness parameter k, frame-to-wall relative stiffness α, and base rotational restraint R_f on RWF system demand. The main conclusions drawn from this study can be summarized as follows:

1) The lateral displacement, shear force, and moment distribution of the RWF system predicted using the proposed solutions agree reasonably well with the numerical analysis results. These solutions can reliably characterize the seismic response of tall RWF systems in the linear-elastic range.

2) The axial deformation of columns increases overall displacement and drift of the RWF system. These effects are more pronounced for higher frame-to-wall stiffness ratios (e.g., $\alpha = 6$), as in this case the frame controls the overall system response. This implies that stiff rocking walls should be employed to control the lateral displacement and drift demands of tall and slender frames.

3) For relatively flexible rocking walls (e.g., $\alpha = 6$), an increase in axial stiffness parameter k results in higher wall shear force and moment, especially near the base. Therefore, models assuming axially-rigid columns can result in nonconservative estimates of wall shear and moment demands.

4) When the base restraint R_f of the rocking wall is increased, the displacements and drifts are reduced in the bottom half and the RWF deforms in a flexural manner. The effects of axial deformation of columns are more pronounced for a RWF system with smaller R_f.

5) Shear force and moment carried by the wall increase markedly with increase in wall base restraint R_f. This additional demand due to base restraint should be considered, together with the force-contribution from axial deformation of columns for the design of rocking walls in RWF systems.

The analytical solution presented herein is useful to study the static behavior of uniform RWF systems. Further research is needed to examine the dynamic response of RWF systems and effect of nonuniform stiffness along the height. Furthermore, the direct-displacement based design method for RWF systemsbased on an equivalent linearization approach can be developed utilizing the proposed solutions.

5. Acknowledgements

The first author would like to express his sincere gratitude to the Ministry of Education, Culture, Sports, Science and Technology (MEXT), Japan for the funding of his Doctoral Studies at Tokyo Institute of Technology. This work was supported by JST Program on Open Innovation Platform with Enterprises (JPMJOP1723), Research Institute and Academia, and the MEXT under Grant-in Aid for Scientific Research (A) No. 16H02373 (PI: Susumu Kono).

6. References

[1] Kurama YC, Sause R, Pessiki S, Lu LW (1999): Lateral load behavior and seismic design of unbonded post-tensioned precast concrete walls. *ACI Structural Journal*, **96**(4), 622-632.

[2] Holden T, Restrepo J, Mander JB (2003): Seismic performance of precast reinforced and prestressed concrete walls. *Journal of Structural Engineering (ASCE)*, **129**(3), 286-296.

[3] Marriott D, Pampanin S, Bull D, Palermo A (2008): Dynamic testing of precast, post-tensioned rocking wall systems with alternative dissipating solutions. *Bulletin of the New Zealand Society for Earthquake Engineering*, **41**(2), 90-103.

[4] Belleri A, Schoettler MJ, Restrepo J, Fleishman, R B (2014): Dynamic behavior of rocking and hybrid cantilever walls in a precast concrete building. *ACI Structural J*ournal, **111**(3), 661-672.

[5] Midorikawa M, Azuhata T, Ishihara T, Wada A (2006). Shaking table tests on seismic response of steel braced frames with column uplift. *Earthquake Engineering & Structural Dynamics*, **35**(14), 1767-1785.

[6] Eatherton MR, Ma X, Krawinkler H, Mar D, Billington S, Hajjar JF, Deierlein GG (2014). Design concepts for controlled rocking of self-centering steel-braced frames. *Journal of Structural Engineering (ASCE)*, **140**(11), 04014082.

[7] Smith T, Ludwig F, Pampanin S, Fragiacomo M, Buchanan A, Deam B, Palermo A (2007). Seismic response of hybrid-LVL coupled walls under quasi-static and pseudo-dynamic testing. In *2007 New Zealand Society for Earthquake Engineering Conference*, Palmerston North, New Zealand.

[8] Qu Z, Wada A, Motoyui S, Sakata H, Kishiki S (2012): Pin-supported walls for enhancing the seismic performance of building structures. *Earthquake Engineering & Structural Dynamics*, **41**(14), 2075-2091.

[9] Pan P, Wu S, Nie X (2015): A distributed parameter model of a frame pin-supported wall structure. E*arthquake Engineering & Structural Dynamics*, **44**(10), 1643-1659.

[10] Rahgozar N, Moghadam AS, Aziminejad A (2018): Continuum analysis approach for rocking core-moment frames. *Journal of Structural Engineering (ASCE)*, **144**(3), 04018006.

[11] Sun T, Kurama YC, Zhang P, Ou J (2018): Linear-elastic lateral load analysis and seismic design of pin-supported wall-frame structures with yielding dampers. *Earthquake Engineering & Structural Dynamics*, **47**(4), 988-1013.

[12] Heidebrecht AC, Smith BS (1973): Approximate analysis of tall wall-frame structures. *Journal of the Structural Division (ASCE)*, **99**(2), 199-221.

[13] Nollet MJ (1991): *Behavior of wall-frame structures* (PhD Thesis). Department of Civil Engineering and Applied Mechanics, McGill University, Montreal, Canada.

[14] Smith BS, Coull A (1991): *Tall Building Structures: Analysis and Design*. John Wiley & Sons, New York.

[15] McKenna F, Scott MH, Fenves GL (2010): Nonlinear finite-element analysis software architecture using object composition. *Journal of Computing in Civil Engineering (ASCE)*, **24**(1), 95-107.

[16] Subedi N (2019): *Lateral load analysis and influence of ground motion duration on seismic performance of rocking wall-frame buildings* (Master's Thesis). Department of Civil and Environmental Engineering, Tokyo Institute of Technology, Tokyo, Japan.

